한국공작기계학회논문집 Vol.17 No.1 2008. 2.
Transactions of the Korean Society of Machine Tool Engineers

Sensor Fusion and Neural Network Analysis for Drill-Wear Monitoring

Kritsada Prasopchaichana*, Oh-Yang Kwon+

(논문접수일 2007. 9. 6, 심사완료일 2007. 10. 24)

센서퓨젼 기반의 인공신경망을 이용한 드릴 마모 모니터링

Kritsada Prasopchaichana* and 권오양+

Abstract

The objective of the study is to construct a sensor fusion system for tool-condition monitoring (TCM) that will lead to a more efficient and economical drill usage. Drill-wear monitoring has an important attribute in the automatic machining processes as it can help preventing the damage of tools and workpieces, and optimizing the drill usage. In this study, we present the architectures of a multi-layer feed-forward neural network with Levenberg-Marquardt training algorithm based on sensor fusion for the monitoring of drill-wear condition. The input features to the neural networks were extracted from AE, vibration and current signals using the wavelet packet transform (WPT) analysis. Training and testing were performed at a moderate range of cutting conditions in the dry drilling of steel plates. The results show good performance in drill- wear monitoring by the proposed method of sensor fusion and neural network analysis.

Key Words : Neural network, Levenberg-Marquardt , sensor fusion, drill wear, tool-condition monitoring

1. Introduction

Tool-condition monitoring (TCM) is an indispensable component for the prevention of the damage in machine tools and workpieces and the optimization of tool usage in the automated machining. Furthermore, under a certain cutting condition, wear development during drilling can reach the unacceptable levels, resulting in the damage of workpieces as well as machine tools and possibly in the production loss. Flank wear is widely used as the indica-

* 인하대학교 대학원 기계공학과
+ 교신저자, 인하대학교 기계공학부 (okwon@inha.ac.kr)
주소: 402-751 인천시 남구 용현동 253

tion of the severity of drill-wear condition. Its progressive process is caused by the intimate frictional contact and the temperature elevated at the interface between the drill and the workpiece. Flank wear can be measured by using the average and the maximum wear land size, V_B and V_{Bmax}, as shown in Fig. 1.

Various methods for tool wear monitoring have been reported in the literature. Most of them are categorized by two main techniques[1-3]. The first is the direct measurement of tool wear using optical methods, which can only be applied when cutting tools are not in process of cutting. The second is the indirect methods which measure the relationship between the tool condition and the signals acquired depending on the sensors used. Among the various sensors used, each sensoring technique has its own advantages and drawbacks with the result that no single technique has proved to be completely reliable over the complex nature of the cutting processes. Therefore, a sensor fusion system which uses more than one sensor is attractive since the loss of sensitivity in one sensor domain can be offset by information from other sensors.

Three sensing techniques of acoustic emission, vibration and current sensoring were used as the input features in the proposed neural network based on sensor fusion for drill wear monitoring.

Acoustic emission (AE) appeared to be one of the most effective indirect monitoring methods. The major advantage of AE monitoring is that the frequency range of AE

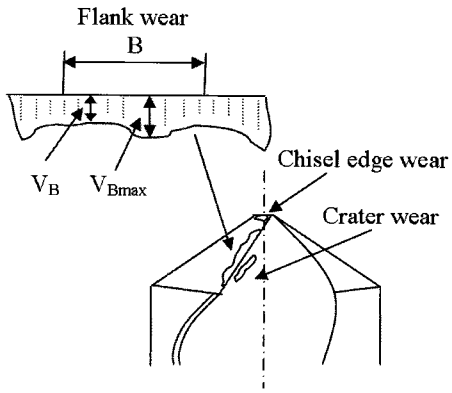

Fig. 1 A schematic of a typical twist drill with flank wear

signals can be much higher than the machine vibrations and environmental noise. In addition, it does not affect the cutting condition. But one of the most important features for AE signal is the additional signal processing which extract signal features from the signals detected under given cutting conditions[3-6]. A more comprehensive monitoring strategy would involve multi-sensor and data fusion technique which will be a more effective approach for AE- based tool condition monitoring[1,7].

Vibration analysis is also employed for drilling. It was found that an increase in drill wear will lead to an increase in the frequency content of the vibrations, particularly in the thrust direction. For tools near failure, the amplitudes of vibrations tend to increase[4]. Vibration signals have tremendous promise for tool wear monitoring and diagnosis using simple structured neural networks[8].

Current sensor is considered one of the most effective means of monitoring tool wear and adaptive control of machining processes. The advantage of using current sensors, which are fitted to the external power supply lines, is that these sensors do not hinder the machining process and are cost effective[4,9]. Both the spindle motor and feed motor current increase as tool wear increase. It is found that the tool wear has more significant effects on the feed motor current than the spindle motor current[3]. Current Sensor signals individually or in combination with other sensors signals can be used as input to a tool condition monitoring system using artificial neural networks.

In this study, we have investigated the feasibility to use signals from multi-sensor sources to train and test the neural networks based on sensor fusion for predicting the drill flank wear. Seven neural network architectures were designed with the different groups of input sensor features. AE and vibration signals were extracted as input features of root-mean-square (RMS) voltages of the decomposed signal by wavelet packet transform (WPT). Both the spindle motor and feed motor current signals were extracted as RMS voltages without WPT signal decomposition.

2. Experimental procedures

Experiments were carried out on a machining center

(HiMac-V100, Hyundai). Drills used were AISI M2 twist drills with 6 mm diameter and point angle of 118°. Workpieces were AISI 1055 steel plates of 120×120×25 mm. The hardness of plates was measured to 215 H_B. Two AE sensors (B1025, Digital Wave) were mounted on the clamping fixture at the opposite side each other as shown in Fig. 2. AE activities during drilling tests were monitored and recorded by using an AE data acquisition board (Mistras2001, Physical Acoustics), with pre-amplification of 40 dB, band-pass filtering at 0.1-1.2 MHz and threshold of 50 dB. A vibration measuring accelerometer (Rectuson model SA12ZSC-T1, with sensitivity of 100 mV/(m/s^2) and a measurement range of ±40 m/s^2) was mounted on the spindle-bearing housing of CNC machining center machine. The analog signals were fed into charge amplifier (MMF model M68D3) with band-pass filter 3 Hz-50 kHz and then to a digital oscilloscope with sampling rate 20,000 samples/s. The spindle motor and feed motor current signals of the machining center were measured with Hall current sensors (HINODE model H-A050A, with sensitivity of 50A/4V) and the signals were sent to a digital oscilloscope with sampling rate 1,000 samples/s.

During each test, flank wear was measured by an optical microscope aided by a digital camera and an image processing software. Drilling tests were first performed at nine sets of cutting conditions with three cutting speeds (22, 26, 30 m/min) and three feed rates (0.13, 0.15, 0.17 mm/rev) without coolant, which were used for off-line training and testing. Three sets of cutting conditions were added later to check the validity of the neural networks with the features extracted from untrained data set. The cutting process was continued until the max. allowable flank wear of V_B = 0.3 mm or the complete failure of a drill.

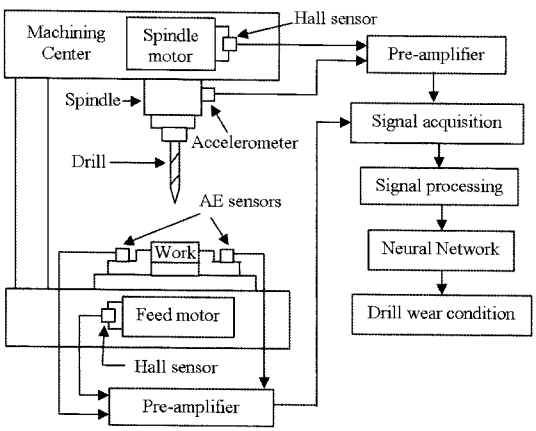

Fig. 2 Schematic diagram of the experiment set-up

3. Signal analysis and feature extraction

In through-hole drilling operation, three steps are distinguishable, which are stage I corresponding to transient drilling or entry stage, stage II called steady drilling stage and the last stage III named exit stage as shown in Fig. 3. For transient drilling stage, the vibration and current signal amplitudes increase with drilling depth until the drill tip completely penetrates the workpiece when the signals become stable. During Stage III, current signal decreases, but vibration signal amplitude increases due to unstable cutting process (incomplete cutting lips). Therefore, the vibration and current signals obtained from beginning of steady drilling stage about 2 seconds were extracted as input features to the neural networks.

AE signal activity also is fluctuated in stage I and III because of high chip-breakage rate and unstable cutting process. Based on the analysis of AE sources, AE signals detected from metal cutting consist of the continuous and the transient signals, which have distinctly different characteristics[1]. Continuous signals are associated with shearing in the primary zone and wear on the tool face and the flank, while transient or burst signals are with either tool fracture or chip breakage. In this study, the

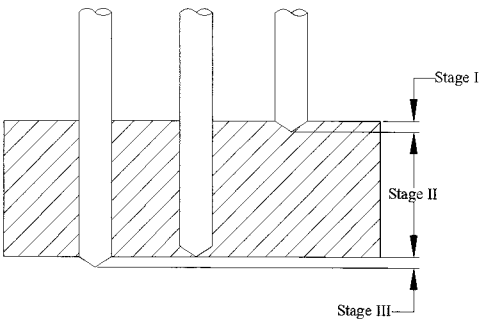

Fig. 3 Three stages of through-hole drilling operation

AE input features to the neural networks were extracted from the continuous AE signals at the beginning of steady drilling stage.

Fig. 4 shows sample AE and vibration signals, their corresponding fast Fouier transform (FFT). The FFT analysis shows that the frequency distribution of signals change magnitude and shift location of spectral peaks as the tool wears. This mean the RMS of signal amplitude is not enough sensitive to the change of tool wear. For a more comprehensive monitoring strategy, the signal should be determined RMS voltages of decomposed components in different time windows and frequency bands by WPT. But in case of current signals, the synchronous spindle and feed motor currents are alternating with a frequency is proportional to the spindle speed and feed rate, respectively as shown in Fig. 5. So, the signal decomposition is unnecessary because signal did not contain various frequencies.

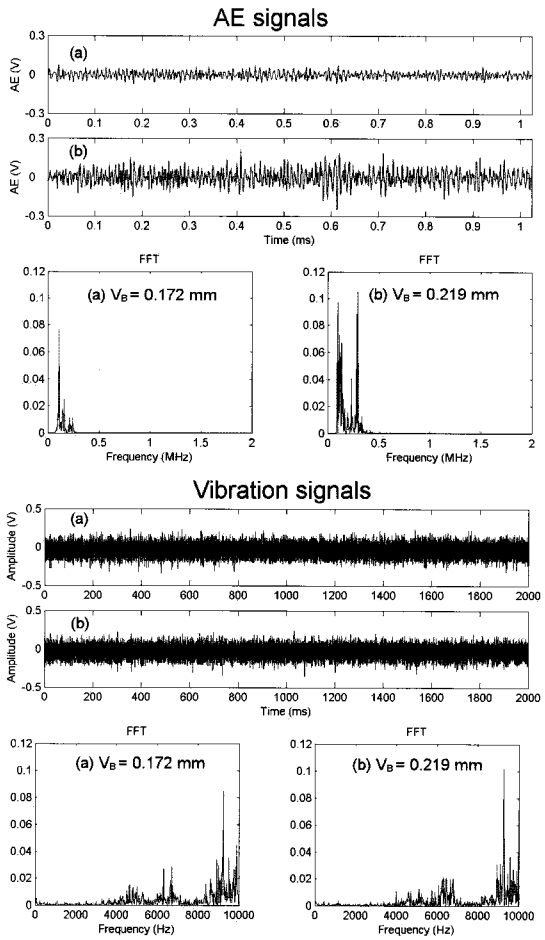

Fig. 4 The AE and vibration signals and their FFT plots for two stages of progressive flank wear, operating at a cutting speed 26 m/min and feed rate 0.13 mm/rev

3.1 Frequency band-RMS analysis based on wavelet packet transform

In wavelet analysis, the signal is decomposed to approximations and details. The approximations are the high-scale, low-frequency components of the signal and the details are the low-scale, high-frequency components. The decomposition process can be iterated, with successive approximations being decomposed in turn, so that one signal is broken down into many lower resolution components. This is called the wavelet decomposition tree[10] as shown in Fig. 6.

In wavelet packet analysis, the details as well as the approximations can be split. Therefore, the wavelet packet method is a generalization of wavelet decomposition that offers a richer range of possibilities for signal analysis. The complete binary tree[10] is produced as shown in the

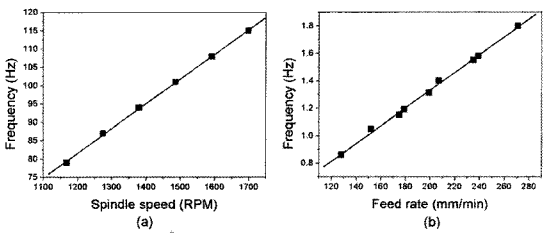

Fig. 5 (a) the relationship between current signal frequency and spindle speed, (b) the relationship between current signal frequency and feed rate

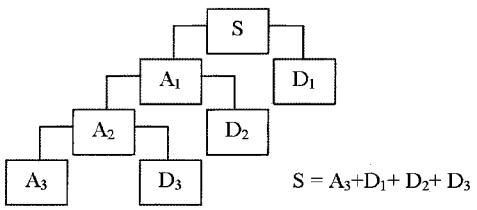

Fig. 6 The 3-level wavelet decomposition tree

following Fig. 7. The idea of this decomposition is to start from a scale-oriented decomposition, and then to analyze the obtained signals on frequency subbands. In this study, the name of wavelet packet are named by numbers of level and order enclosed in parentheses, for example, the wavelet packet AAA_3, DAA_3, ..., and DDD_3 are named wavelet packet (3,0), (3,1), ..., and (3,7) respectively.

MATLAB was used for the wavelet packet transform of AE and vibration waveforms because it provides a versatile wavelet toolbox and also offers the possibility of programming. After AE and vibration waveforms were loaded into MATLAB, wavelet pack transform was carried out to decompose the original signal into its wavelet packets. Decomposition was based on 'db20' wavelet (a member of the Daubechies wavelets family) and three levels for vibration signal and four levels of analysis for AE signal. Each vibration signal was decomposed to 8 wavelet packets, namely wavelet packet (3,0), (3,1), ..., (3, 15) which represent the frequency band [0-1.25], [1.25-2.5], ..., [8.75-10] kHz, respectively as shown in Fig. 8. Because the vibration signals were acquired at sampling rate of 20 kHz, frequencies up to 10 kHz were considered.

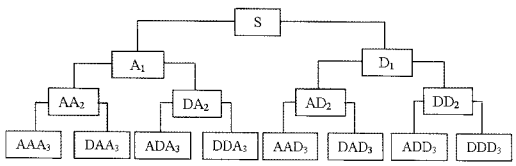

Fig. 7 Wavelet packet decomposition tree at level 3

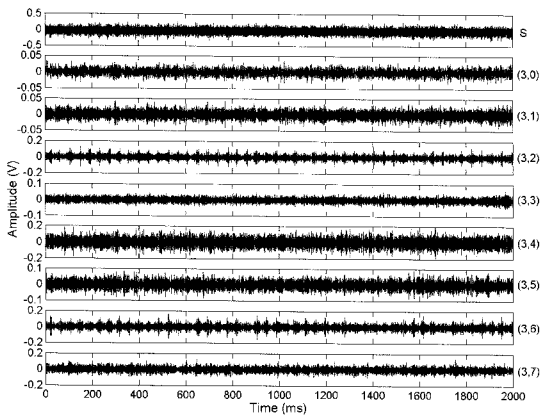

Fig. 8 Three-level wavelet packet decomposition of a vibration signal

For AE signal, each signal was decomposed to 16 wavelet packets, namely wavelet packet (4,0), (4,1), ..., (4, 15) which represent the frequency band [0-125], [125-250], ..., [1875-2000] kHz, respectively. Frequencies up to 2 MHz were considered because the AE signals were acquired at sampling rate of 4 MHz. Obviously, the wavelet packet (4,0), (4,1), ..., (4,7) corresponds to the frequency band of 0-1000 kHz which covers the AE signal frequency in this study and were used for signal decomposition. The family of Daubechies wavelets was chosen because it compactly supports orthonormal wavelets, thus making wavelet packet analysis practicable[10]. The RMS of each frequency band-packet was used to describe the changing feature of the AE and vibration signals which are influenced by the wear size and cutting conditions[2,11].

4. Neural networks

Neural networks are non-linear mapping models that are organized in layers each consisting of neurons, which are linked by weighed connections. In this approach the relationships between input and output variables are developed through a training process in which sets of inputs are applied to the network and the resulting sets of outputs are compared with known correct values. The training data set is cycled through the network until the error is less than an acceptable value. The trained networks are used to predict outputs of inputs which are not used in the training phase.

The architecture of a three-layer feed-forward neural network[8,9,12] was used in this study. This neural network used a hyperbolic-tangent sigmoid transfer function, which is a good trade off for the neural networks where speed is important and the exact shape of the transfer function is not[13]. In this study, the Levenberg-Marquardt algorithm is used in training neural networks in order to obtain neural networks with good generalization capability. This algorithm appears to be the fastest method for training moderate-sized feed-forward neural networks[13]. The

learning process was stopped (i.e., neural network had converged) when the calculated output values were close to the desired target values within an acceptable mean-square error (MSE) value ($MSE < MSE_{goal} = 10^{-5}$).

Seven neural network architectures, shown in Fig. 9, were designed as follows:

1. NN-AE: Input 16 wavelet packet-RMS values of AE signals from two AE sensors and cutting conditions.
2. NN-V: Input 8 wavelet packet-RMS values of vibration signals and cutting conditions.
3. NN-C: Input 2 signal-RMS values of spindle and feed motor currents and cutting conditions.
4. NN-AE-V: Input 16 wavelet packet-RMS values of AE signals, 8 wavelet packet-RMS values of vibration signals and cutting conditions.
5. NN-AE-C: Input 16 wavelet packet-RMS values of AE signals, 2 signal-RMS values of spindle and feed motor currents and cutting conditions.
6. NN-V-C: Input 8 wavelet packet-RMS values of vibration signals, 2 signal-RMS values of spindle and feed motor currents and cutting conditions.
7. NN-All: Input all of features extracted from all sensors and cutting conditions.

5. Results and discussion

The tool wear curve in Fig. 10 shows patterns of the flank wear at different cutting speeds and feeds, as a function of cutting length. The cutting length is the accumulated depth of holes drilled during each test. The V_B values show faster flank wear and shorter drill life with higher cutting speed and feed. However, the relationship among the AE signals, vibration signals, current signals and drill wear was not simple. Therefore the drill wear estimated from the extracted features of all sensor signals were analyzed by neural networks which are non-linear mapping models. Based on the aforementioned neural network model for this study, number of neurons to be used in the hidden layer of a neural network is critical in order to avoid underfitting and overfitting problem. There is no single rule to determine the optimum number of neurons in the hidden layer required for optimum performance. However, number of hidden layer neurons is usually found with trial-and-error approach[8,9,12].

In this study, the number of neurons in hidden layer was determined by a trial-and-error approach. Each network architecture was testified for the average MSE of 10 trials with the number of neurons from one(1) to twenty-five (25) and the minimum value out of 25 average MSE determined the number of neurons. The number of neurons for trial and error was set at the maximum value of 25 because the use of more processing elements in the hidden layer not only required a larger number of training iterations to converge but also added additional CPU load for the tool failure diagnosis in real-time analysis. The Fig. 11 shows the minimum average MSE at the number of hidden neurons 12, 7 and 5 for architectures of NN-AE, NN-V and NN-C, respectively. Similar approach was repeated for other neural network architectures to determine

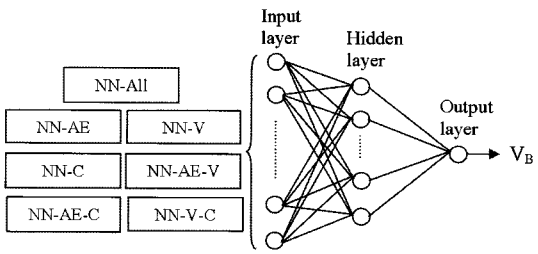

Fig. 9 Seven neural network architectures

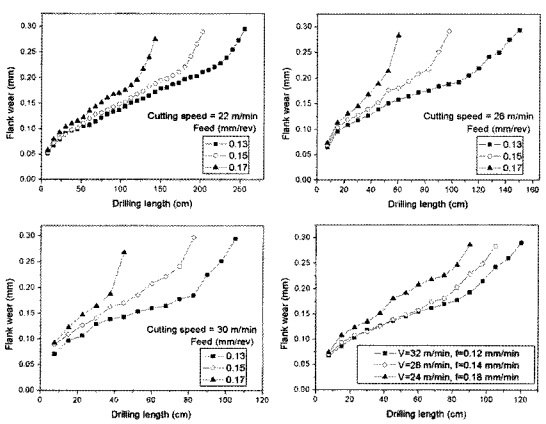

Fig. 10 Drill flank wear size measured during complete useful life

the number of hidden layer neurons. Consequently, the number of hidden neurons 20, 13, 10 and 22 were chosen for architectures of NN-AE-V, NN-AE-C, NN-V-C and NN-All, respectively.

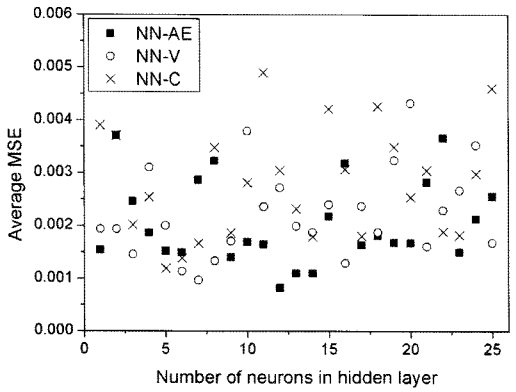

Fig. 11 Average MSE values of neural network architectures NN-AE, NN-V and NN-C as a function of the number of neurons in the hidden layer

Table 1 shows a summary of the performance of the neural networks with different architectures during testing phase in terms of percentage of correct prediction. The testing phase helps the neural network architectures to generalize and increase its declaration accuracy. The results indicated that neural networks with input features extracted from two or three types of sensors were more accurate than the networks with individual sensor input. The overall average correct predictions indicated that the best performance was obtained by the neural network architecture with input features from AE and vibration sensors, i.e. NN-AE-V. The performance of the architecture with input features by AE and current sensors was slightly higher than that by vibration and current sensors, but the difference was almost negligible and within the range of statistical error bound.

In order to further verify the feasibility of using neural networks for the diagnosis of drill wear, the seven architectures were tested with untrained data sets that were

Table 1 Performance of neural networks with different architectures in the testing phase

Drilling conditions		Percentage of correct predictions						
Cutting speed (m/min)	Feed (mm/rev)	NN-AE	NN-V	NN-C	NN-AE-V	NN-AE-C	NN-V-C	NN-All
22	0.13	79.58	82.55	80.69	88.26	85.93	82.71	86.25
22	0.15	82.41	81.70	81.47	92.15	87.82	85.18	90.73
22	0.17	87.17	86.19	85.53	91.48	93.45	83.34	88.68
26	0.13	81.96	79.56	81.20	91.88	81.48	82.35	91.27
26	0.15	88.25	86.66	88.28	90.16	90.76	85.17	94.36
26	0.17	88.74	85.92	86.42	95.88	92.24	89.37	93.39
30	0.13	89.58	85.95	84.38	97.41	86.65	91.66	93.57
30	0.15	85.08	82.11	85.58	96.51	88.52	88.02	85.55
30	0.17	90.16	89.68	82.04	96.58	92.69	91.42	93.92
Average		86.67	83.83	83.95	93.37	88.36	86.58	90.86
24*	0.18*	83.41	86.44	72.67	95.14	80.10	83.32	86.76
28*	0.14*	87.68	80.89	79.53	89.35	92.18	83.36	90.58
32*	0.12*	85.58	79.04	79.44	94.64	83.89	87.74	91.44
Average*		85.56	82.12	77.21	93.04	85.39	84.81	89.60
Overall average		86.37	83.36	82.27	93.28	87.55	86.14	90.54

*Untrained data sets; Signals from these conditions were not used in the training phase

acquired under the drilling conditions different from those used for training the neural networks. The performance of all architectures except NN-C was satisfactory, although it was less accurate than the performance for the cutting conditions used for training. The neural network architecture with individual current sensor input, not only obtained the lowest performance, but the difference in the percentage of correct prediction between trained and untrained also became much larger. Because the line voltage of power supply might not be constant throughout the experiment due to the line voltage might change over time to time in the shop floor where the machining was carried out. This point also caused the architecture of NN-All not to obtain the best performance in this study, even though the extracted features from AE and vibration signals offset the loss of sensitivity in current sensor domain. This indicated that the percentage of correct prediction was not increased with the number of sensor fusion, with rather depending on the sensitivity of signal input with proper feature extraction method.

6. Conclusion

A multi-layer feed-forward neural network with Levenberg-Marquardt training algorithm was developed and applied to sensor fusion system to be used for drill-wear monitoring. The performance of seven different neural network architectures was tested and found to be sensitive to the type of input data. The neural networks with input features extracted from sensor fusion were more accurate than the networks with individual sensor input. The sensor fusion of AE and vibration signal features extracted by RMS-WPT analysis as the input resulted in the best performance at a correct drill wear prediction of 93%. In addition, the performance of neural network based on sensor fusion was not increased with the number of sensor fusion, with rather depending on the extracted feature of signals input which optimally offset the loss of sensitivity to each other. The results showed that once the neural network was properly trained, it could be a powerful and reliable tool to solve the classification and pattern recognition problems of such sensor fusion as being acquired in the tool-condition monitoring applications.

Acknowledgement

This work was supported by Inha University Research Grant (INHA-31635).

References

(1) Li, X., 2002, "A brief review: acoustic emission method for tool wear monitoring during turning," *Int. J. Mach. Tools Manufact.*, Vol. 42, pp. 157~165.

(2) Li, X. and Wu, J., 2000, "Wavelet analysis of acoustic emission signals in boring," *Proc. Instn. Mech. Engrs. Part B*, Vol. 214, No. 5, pp. 421~424.

(3) Jantunen E., 2004, "The applicability of various indirect monitoring methods to tool condition monitoring in drilling," *Int. J. COMADEM*, Vol. 7, No. 3, pp. 24~31.

(4) Rehorn, A. G., Jiang, J. and Orban, P. E., 2005, "State-of-the-art methods and results in tool condition monitoring: a review," *Int. J. Adv. Manufacturing Technology*, Vol. 26, pp. 693~710.

(5) Sun, J., Hong, G. S., Rahman, M. and Wong, Y. S., 2004, "Identification of feature set for effective tool condition monitoring by AE sensing," *Int. J. Production Research*, Vol. 42, No. 5, pp. 901~918.

(6) Shin, H. G., Kim, S. I. and Kim, T. Y., 2001, "A Study on Tool Wear in Drilling of Hot-rolled High Strength Steel," *Korean Society of Machine Tool Engineer*, Vol. 10, No. 2, pp. 10~17.

(7) Lim, J. S., Wang, D. H., Kim, W. I. and Lee, Y. K., 2002, "The estimation of tool wear and fracture mechanism using sensor fusion in micro-machining," *Proceedings of the Korean Society of Machine Tool Engineers Conference*, pp. 245~250.

(8) Abu-Mahfouz, I., 2003, "Drilling wear detection and classification using vibration signals and artificial neural network," *Int. J. Mach. Tools Manufact.*, Vol. 43, pp. 707~720.

(9) Patra, K., Pal, S. K. and Bhattacharyya, K., 2007, "Artificial neural network based prediction of drill

flank wear from motor current signals," *Applied Soft Computing*, Vol. 7, pp. 929~935.

(10) Misiti, M., Misiti, Y., Oppenheim, G. and Poggi J. M., 2000, *Wavelet Toolbox User's Guide, Version 2.0*, Natick, MA, USA, The Math Works, Inc.

(11) Kim, J. S., Kim, N. K. and Bae, J. K., 1997, "Monitoring of Tool Wear using AE Signal in Interrupted cutting," *Korean Society of Machine Tool Engineer*, Vol. 6, No. 2, pp. 112~118.

(12) Singh, A. K. and Panda, S. S., 2006, "Predicting drill wear using an artificial neural network," *Int. J. Adv. Manuf. Technol.*,Vol. 28, pp.456~462.

(13) Demuth, H. and Beale, M., 1998, *Neural Network Toolbox User's Guide, Version 3.0*, Natick, MA, USA, The Math works, Inc.